Conformation of Magainin-2 and Related Peptides in Aqueous Solution and Membrane Environments Probed by Fourier Transform Infrared Spectroscopy†

Michael Jackson,‡ Henry H. Mantsch,*,‡ and John H. Spencer§

Institute for Biodiagnostics, National Research Council of Canada, Winnipeg, Manitoba R3B 1Y6, Canada, and Department of Biochemistry, Queens University, Kingston, Ontario K7L 3N6, Canada

Received February 26, 1992; Revised Manuscript Received May 15, 1992

ABSTRACT: The conformational properties of the magainin family of antimicrobial peptides in aqueous solution and in model membranes have been probed by Fourier transform infrared spectroscopy. The magainins were found to be structureless in aqueous solution at neutral pD, confirming other studies by Raman and circular dichroism spectroscopy. Increasing the pD to 10 induced the formation of predominantly α-helical secondary structures, with some β-sheet. In the presence of negatively charged liposomes (dimyristoylphosphatidylglycerol), the peptides folded into α-helical secondary structures with some β-sheet structure evident. On the other hand, in the presence of zwitterionic phospholipids (dimyristoylphosphatidylcholine), the spectra were identical to those in aqueous solution. For some magainins, the interaction with charged liposomes was modulated by the presence of cholesterol; cholesterol was found to promote the formation of β-sheet structures, as evidenced by the appearance of amide I bands at 1614 and 1637 cm^{-1}. Differences in structure were observed between the amidated and nonamidated forms of some peptides. From the data, a mechanism of antimicrobial action of the magainin family of peptides is proposed.

The magainins are a family of positively charged antimicrobial peptides which include magainin-1 (MGN-1)[1] magainin-2 (MGN-2), a peptide with an amino-terminal glycine and a carboxy-terminal leucine amide (PGLa), xenopsin precursor fragment (XPF), caerulin precursor fragment (CPF), and levitide precursor fragment (LPF) (Bevins & Zasloff, 1990). The antimicrobial activity of magainins was first identified in skin extracts of the African clawed frog *Xenopus laevis* (Zasloff, 1987). The amino acid sequence was identical to that of a peptide PGS (Giovannini et al., 1987) which had previously been identified as one of the numerous peptide components of *Xenopus laevis* skin granular gland secretions which also include PGLa, xenopsin, caerulin, XPF, and CPF (Gibson et al., 1986; Bevins & Zasloff, 1990).

The small size of the magainin family of peptides (21–35 amino acids, see Table I for structures of MGN-2a, PGLa, and XPFa) and the availability in milligram quantities through chemical synthesis provided an opportunity for a series of structural and physiological studies. A helical wheel representation (Zasloff, 1987; Duclohier et al., 1989) revealed the amphipathic potential of MGN-1 which in turn indicated the potential for a membrane-based action. Similar projections were proposed for CPF and XPF by Gibson et al. (1986). Synthetic lipid bilayer patch-clamp studies showed that MGN-1 and MGN-2 form anion channels (Duclohier et al., 1989), supporting the hypothesis of a membrane-related activity. In view of the positive charge carried by all members of the magainin family of peptides at physiological pH, this membrane activity would be expected to be expressed against negatively charged membranes. Circular dichroism, Raman, and nuclear magnetic resonance spectroscopic studies (Chen et al., 1988; Marion et al., 1988; Duclohier et al., 1989; Matsuzaki et al., 1989; Williams et al., 1990) demonstrated an α-helical conformation for maginin-1 and the amidated form of magainin-2 (MGN-2a) in the presence of trifluoroethanol and acidic phospholipids.

Table I: Amino Acid Sequences of Three Magainins

MGN-2a	Gly-Ile-Gly-Lys-Phe-Leu-His-Ser-Ala-Lys-Lys-Phe-Gly-Lys-Ala-Phe-Val-Gly-Glu-Ile-Met-Asn-Ser-NH_2
PGLa	Gly-Met-Ala-Ser-Lys-Ala-Gly-Ala-Ile-Ala-Gly-Lys-Ile-Ala-Lys-Val-Ala-Leu-Lys-Ala-Leu-NH_2
XPFa	Gly-Trp-Ala-Ser-Lys-Ile-Gly-Glu-Thr-Leu-Gly-Lys-Ile-Ala-Lys-Val-Gly-Leu-Lys-Glu-Leu-Ile-Glu-Pro-Lys-NH_2

From the facts presented above, it appears possible that the antimicrobial activity of magainins may be related to the adoption of a helical structure upon charge neutralization at the surface of a negatively charged bilayer, followed by insertion of the helix into the bilayer-forming pores. The correlation between antimicrobial activity and helical structure is supported by the observation of an enhanced antimicrobial activity of synthetic magainin analogues which had more α-helical potential (Chen et al., 1988, 1990; Juretic et al., 1989; Williams et al., 1989; Cuervo et al., 1990).

MGN-1, MGN-2, XPF, and CPF are secreted from the granular glands with unmodified carboxy termini. PGLa, on the other hand, is secreted as the carboxy-amidated peptide. Most studies on magainins to date have used the amidated form of the peptides, sometimes to take advantage of the increased resistance to proteases of this form (Juretic et al., 1989). Unfortunately, data on the amidated and nonamidated peptides are not directly comparable, especially those involving charged interactions. In the present study, we have used infrared spectroscopy to study the structure of MGN-2, MGN-2a, XPFa, PGL, and PGLa, both in aqueous solution and in a membrane environment. Our findings support a membrane insertion-based mechanism for the antimicrobial action of these peptides.

† The studies at Queens University were supported by a grant from the School of Graduate Studies and Research.

* Address correspondence to this author.

‡ National Research Council of Canada.

§ Queens University.

[1] Abbreviations: FT-IR, Fourier transform infrared; DMPG, dimyristoylphosphatidylglycerol; DMPC, dimyristoylphosphatidylcholine; DMPA, dipalmitoylphosphatidic acid; MGN-2, magainin-2; MGN-2a, magainin-2 amide; PGL, peptide glycylleucine; PGLa, peptide glycylleucine amide; XPF, xenopsin precursor fragment; XPFa, xenopsin precursor fragment amide.

0006-2960/92/0431-7289$03.00/0

MATERIALS AND METHODS

Synthetic MGN-2a, XPFa, and PGLa were the generous gifts of Dr. M. Zasloff. Their synthesis has been described elsewhere (Zasloff et al., 1988; Soravia et al., 1988). MGN-2 and PGL were synthesized in the Core Facility for Protein/DNA Chemistry, Department of Biochemistry, Queens University at Kingston, on an Applied Biosystems Model 431A automated peptide synthesizer. The peptides were assembled stepwise on a preloaded Wang resin (Aminotech), cleaved from the solid support using a cleavage cocktail (King et al., 1990), precipitated in ether, and lyophilized. Purity was determined by reverse-phase HPLC on a Waters 600E system.

Dimyristoylphosphatidylglycerol (DMPG) and dimyristoylphosphatidylcholine (DMPC) were purchased from Sigma Chemical Co. (St. Louis, MO). Cholesterol was from Fluka.

Samples for FT-IR spectra were prepared as follows. For solution spectra, peptides were dissolved to a final concentration of 10 mM in 50 mM Tris, pD 5, 7, or 10. For samples in the presence of lipid, the peptide was added to liposomes to give a molar ratio of 20:1 (lipid to protein) and a final peptide concentration of 10 mM. For experiments with lipid and cholesterol, lipid and cholesterol were dissolved in the required ratios in chloroform/methanol 2:1, the solvent was evaporated under nitrogen, and the samples were left under vacuum overnight to remove final traces of solvent. Liposomes were formed by the addition of 50 mM Tris followed by sonication. Sufficient peptide was added to maintain lipid:peptide ratios at 20:1.

For each sample, 3 μL was placed between a pair of CaF_2 windows separated by a 50-μm Mylar spacer and mounted in a Harrick demountable cell. Temperature was maintained by a circulating water bath. Spectra were recorded on a Digilab FST-60 FT-IR spectrometer equipped with a DTGS detector and continuously purged with dry nitrogen. For each sample, 100 interferograms were collected and Fourier-transformed to generate a spectrum at 2-cm^{-1} resolution. Absorbance spectra were generated by digital subtraction of buffer spectra recorded under identical conditions. The infrared spectra in Figures 1–4 are shown after band-narrowing by Fourier self-deconvolution by use of a band-narrowing factor of $k = 1.7$ and half-bandwidths of 13.5 cm^{-1} (Mantsch et al., 1988).

Antibacterial activity was measured using *Escherichia coli* K12, strain D31, obtained from Dr. D. L. MacDonald, Magainin Sciences Incorporated. Cells were grown in Luria broth (LB) to mid-log phase. LB agar plates were overlaid with 3.5 mL of 0.7% top agar inoculated with 10^8 log-phase cells. Holes (wells) 2 mm in diameter were punched out of the top agar layer with a sterile Pasteur pipet and the requisite volumes of antibacterial peptide solutions pipetted into the wells. The plates were incubated for 3 h at 37 °C and the diameters of the clear area devoid of bacterial growth measured.

RESULTS

Antibacterial Activity. The results of antibacterial testing upon *E. coli* K12, strain D31 are shown in Table II. The antibacterial activities of the peptides are within previously described limits (Zasloff et al., 1988; Soravia et al., 1988) with XPF the most active.

IR Spectra of Amidated Peptides. The amide I region of the IR spectrum of PGLa in aqueous (^2H_2O) solution at two different pD values is shown in Figure 1A. At acidic and neutral pD, the amide I maximum occurred at ~1643 cm^{-1}, a position characteristic of proteins and peptides which have little or no well-defined secondary structure. Solvent accessibility and the degree and strength of hydrogen bonding may be inferred from the rate of disappearance of the amide II band at around 1550 cm^{-1} (predominantly an N–H bending vibration) in ^2H_2O. Complete proton–deuteron exchange was achieved immediately upon dissolution as indicated by the complete disappearance of the amide II band (not shown). Elevation of the pD to 10 resulted in a shift in the amide I maximum to 1648 cm^{-1}. Similar spectra and pD dependencies were obtained for XPFa and MGN-2a.

Table II: Minimal Peptide Concentration Required for Inhibition of *E. coli* Growth

clear growth area (diameter in mm)	peptide concn (μg/mL)				
	MGN-2	MGN-2a	PGL	PGLa	XPFa
4	20.7		21	nd[a]	nd
5	27.6	16.4	28	nd	nd
6		24.6			nd
7		32.8		18	7.5

[a] Not determined.

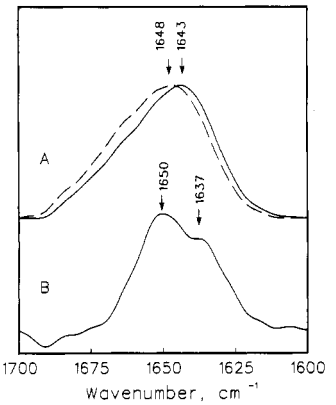

FIGURE 1: (A) IR spectra in the amide I region of PGLa in ^2H_2O solution, pD 5 (solid line) and 10 (dashed line). (B) IR spectrum of MGN-2a in the presence of DMPG at 15 °C.

In the presence of DMPG at 15 °C (below the phase transition of the lipid) at pD 7, the amide I maximum of MGN-2a was seen at 1650 cm^{-1}, with a second band at 1637 cm^{-1} (Figure 1B). A small but reversible increase in frequency of the main component to 1651 cm^{-1} was seen upon increasing the temperature to 25 °C, with a reduction in the intensity of the 1637-cm^{-1} component. Similar results were found for XPFa (not shown). The amide I maximum for PGLa was observed at 1646 cm^{-1}, with a second band at 1632 cm^{-1}. Elevation of the temperature above the phase transition resulted in a reversible and consistently observed increase in the amide I frequency to 1648 cm^{-1} with a decrease in the intensity of the 1632-cm^{-1} band.

Spectra of PGLa in the presence of DMPG/cholesterol are shown in Figure 2A. Major absorptions were seen at 1647, 1628, and 1614 cm^{-1}, the intensity of the 1614-cm^{-1} band being proportional to the cholesterol content. The strong band at 1673 cm^{-1} arises from the counterion trifluoroacetate often found in synthetic peptides because of the use of trifluoroacetic acid (Surewicz & Mantsch, 1989). Spectra of MGN-2a and XPFa in DMPG/cholesterol mixtures at 1:1, 2:1, and 10:1 molar ratios were identical to those in DMPG without cholesterol. Spectra of all three peptides in the presence of DMPC and DMPC/cholesterol at pD 7 were similar to those obtained in aqueous solution at pD 7, with amide I maxima at 1642–1644 cm^{-1} (spectra not shown).

Figure 2B shows the spectrum of PGLa in the presence of 5 mM SDS. The major amide I band was seen at 1650 cm^{-1} with a second band at 1637 cm^{-1}. A rather unusual feature of this spectrum was the drastic reduction in the intensity of the amide I band, as judged from the decrease in the ratio of

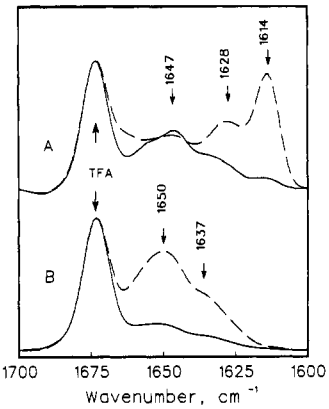

FIGURE 2: (A) Infrared spectra in the amide I region of PGLa in the presence of DMPG/cholesterol at 10:1 (solid line) and 1:1 molar ratios (dashed line). (B) IR spectra of PGLa in 5% SDS in ^2H_2O (solid line) and 5% SDS/100 mM cholesterol (dashed line).

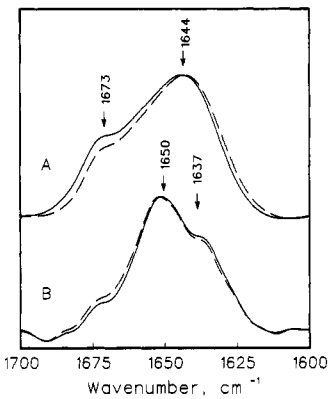

FIGURE 3: (A) IR spectra in the amide I region of MGN-2 at pD 5 (solid line) and pD 10 (dashed line). (B) IR spectra of MGN-2 in the presence of DMPG at 15 °C (solid line) and 25 °C (dashed line) in the amide I region.

the peak height of the trifluoroacetate band (used in these spectra as a marker band) to that of the amide I band. A similar result was obtained in the presence of DMPA (dimyristoylphosphatidic acid). Magainin-2a and XPFa showed bands in similar positions in SDS and in the presence of DMPA, although no reduction in intensity was apparent. In the presence of SDS/cholesterol (1:1) or DMPA/cholesterol (1:1), spectra of MGN-2a and XPFa were identical to those in the absence of cholesterol. However, for PGLa, the reduction in intensity seen in the presence of SDS and DMPA was reversed by the incorporation of cholesterol.

IR Spectra of Nonamidated Peptides. The spectrum of MGN-2 without the C-terminal amide group is shown in Figure 3A. At acidic pD, the amide I maximum was seen at 1644 cm^{-1}, decreasing to 1643 cm^{-1} at pD 10. A shoulder at 1673 cm^{-1} in Figure 3 is again attributed to trifluoroacetate contamination. A similar trend was seen with PGL, the nonamidated form of PGLa.

The spectrum of MGN-2 in the presence of DMPG at 15 °C is shown in Figure 3B. The amide I maximum is at 1650 cm^{-1} with another band at 1637 cm^{-1}. Elevation of the temperature to 25 °C resulted in a small but reproducible increase in the amide I frequency to 1651 cm^{-1} together with a decrease in the intensity of the shoulder at 1637 cm^{-1}. Similar results were obtained with PGL in DMPG, where the amide I maximum was seen at 1648 cm^{-1} with a shoulder at 1637 cm^{-1} (Figure 4A). Increasing the temperature to 25 °C resulted in a small reproducible increase in frequency to 1649 cm^{-1} with a decrease in intensity at 1637 cm^{-1}. For both peptides, the increase in frequency above the phase transition of the lipid was reversed upon cooling.

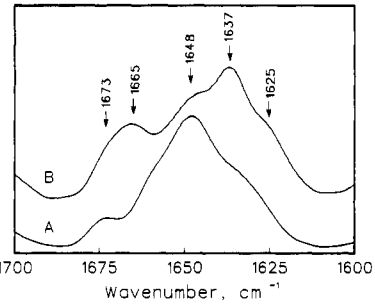

FIGURE 4: IR spectra in the amide I region of PGL in the presence of DMPG (A) and DMPG/cholesterol 1:1 (B).

In the presence of DMPG/cholesterol, IR spectra of MGN-2 were identical to those obtained in the presence of DMPG alone. Addition of PGL to DMPG bilayers containing cholesterol produced an amide I maximum at 1637 cm^{-1}, with additional features at 1648, 1665, and 1625 cm^{-1} (Figure 4B).

DISCUSSION

The magainin family are low molecular weight, amphipathic, positively charged peptides which exhibit a broad-spectrum antibacterial, antifungal, and antiprotozoan activity at concentrations which do not cause hemolysis (Zasloff, 1987; Zasloff et al., 1988; Soravia et al., 1988). The amphipathic nature of the peptides has led to suggestions that this antimicrobial activity is the result of interactions with the microbial cell membrane, forming pores or channels (Zasloff, 1987; Zasloff et al., 1988; Giovannini et al., 1987; Duclohier et al., 1989; Westerhoff et al., 1989; Juretic et al., 1989; Williams et al., 1990). We have undertaken this study to assess the conformation of MGN-2a, MGN-2, PGLa, PGL, and XPFa in solution and in the membrane environment.

As a prerequisite to any comparative structural study, it was necessary to determine whether or not the peptides to be used were fully functional. Antibacterial assays on *E. coli* K12, strain D13, showed the synthetic peptides to be as potent as the natural forms and synthetic peptides used by others. The data revealed that XPFa was the most potent, exhibiting activity twice that of PGLa and 4 times that of MGN2a. MGN and PGL were equipotent.

Raman (Williams et al., 1990) and circular dichroism spectroscopic studies (Chen et al., 1988; Matsuzaki et al., 1989) have shown that magainins have little regular structure in aqueous solution at neutral pD, a finding confirmed by the present IR spectroscopic data (Figure 1A). The amide I maximum at 1642–1644 cm^{-1} for MGN-2a, PGLa, and XPFa at pD 5–7 is typical of a protein with little long-range order [all assignments in this work are based on Byler and Susi (1987), Surewicz and Mantsch (1988), and Jackson et al. (1989)]. Furthermore, the broad, featureless nature of the amide I band and the complete deuteration of the peptide (as evidenced by the absence of an amide II absorption) also suggested that the peptide lacks long-range order, which may be considered to arise from charge repulsion between the numerous lysine residues.

The lack of long-range order in PGLa suggested by the FT-IR spectrum is in conflict with the Raman data of Williams et al. (1990), who found the structure to be predominantly β-sheet (63%) and turns (21%) under these conditions. However, this result probably reflects aggregation of the peptide in the Raman study. Aggregation of proteins and peptides is often accompanied by the formation of intermolecular hydrogen bonds, forming an intermolecular β-sheet. Such structures may be mistaken for intramolecular β-sheets.

Deprotonation of the lysine residues may be expected to result in a more compact, folded conformation for the peptides. The position of the amide I maximum of MGN-2a, PGLa, and XPFa at pD 10 (1647–1650 cm^{-1}) indicated that under these conditions an α-helix is the preferred conformation.

While PGLa is the form of this peptide found in frog skin exudates (Andreu et al., 1985), MGN-2 is secreted with a free carboxy terminus (Zasloff, 1987). It was therefore relevant to study the structure of the nonamidated forms of the peptides. Surprisingly, the replacement of the amide group with a carboxylate group significantly altered the pD dependence of the FT-IR spectra (Figure 3A). No helical structures were apparent at high pD for PGL or MGN-2; rather, it appears that increasing the pD decreases the amide I frequency compared to the frequency seen at acidic pD. The reason for this unexpected result is not clear.

Each of the peptides studied carries a net positive charge, and as such would be expected to interact with negatively charged lipids. As shown in Figures 1B and 3B, each peptide undergoes significant conformational rearrangements when added to suspensions of DMPG. An increase in the amide I frequency to 1647–1650 cm^{-1} indicates that upon binding to DMPG bilayers at 15 °C helical secondary structures are induced. This is presumably the result of charge neutralization, which will allow the peptides to fold into a more compact and favorable structure. Additional features in the spectral range 1632–1637 cm^{-1} indicate that some β-sheet secondary structures are formed. Absorptions in this spectral region have also been attributed to 3_{10}-helices, mainly upon empirical grounds (Prestrelski et al., 1991). However, recent studies (Kennedy et al., 1991) have shown that peptides known to adopt a 3_{10}-helical structure exhibit absorptions in organic solvents at frequencies higher than those of the α-helix (in the range 1660–1666 cm^{-1}) rather than lower. This is to be expected, due to the distortions of the helical hydrogen-bonding network. In addition, 3_{10}-helices are usually minor structural elements within proteins and peptides, in contrast to the significant intensity reported here at 1632–1637 cm^{-1}. For these reasons, we assign absorptions in this region to β-sheet. For MGN-2a, these results agree well with Raman studies (Williams et al., 1990). However, the data for PGLa conflict with the Raman results which found a predominantly β-sheet and turn structure for PGLa in DMPG bilayers. Again, this probably reflects aggregation of the peptide.

While the IR results indicate that each peptide adopts an α-helical configuration in the presence of DMPG, it is not possible to say whether the helices are held at the membrane surface by electrostatic attractions or whether they penetrate the bilayer. It has been suggested from Raman studies that MGN-2a binds to the surface rather than spanning the bilayer (Williams et al., 1990). This is unlikely for three reasons. First, if an amphipathic helix is to be held at the surface of a bilayer, it requires the polar face to interact with the charged headgroup. In turn, this requires that the apolar face be exposed to the solvent, which would be energetically unfavorable. Second, it has been demonstrated that a reversible increase in α-helicity of the peptides occurred upon increasing the temperature above the T_m of the bilayer. Such a change would not be expected if the peptides were held at the bilayer surface. Finally, it has been demonstrated by IR spectroscopy that incorporation of MGN-2a into bilayers of *Salmonella typhimurium* lipopolysaccharide resulted in disruptions of the bilayer packing, suggesting peptide insertion (Rana et al., 1990). We suggest that the peptide partially penetrates into the bilayer below the T_m, with the portion of the peptide outside the bilayer in a β-sheet configuration. Increasing the disorder of the bilayer allows the peptide to penetrate further into the bilayer, with an increase in helicity at the expense of β-sheet.

The peptides studies here have been demonstrated not to show hemolytic activity at antimicrobial concentrations (Bevins & Zasloff, 1990). This is presumably related to the difference in the composition of microbial and animal cell membranes. Animal cell membranes have little negatively charged lipid in the outer layer of the bilayer, which is composed predominantly of phosphatidylcholines, while bacterial cell membranes are composed predominantly of phosphatidylglycerols. In addition, animal cell membranes contain appreciable amounts of cholesterol. Thus, the interaction of each peptide with DMPC, DMPC/cholesterol, and DMPG/cholesterol was studied.

In the presence of DMPC and DMPC/cholesterol, each peptide exhibited spectra identical to those seen in aqueous solution at neutral pD, indicating no interaction with the bilayer. This is not surprising considering the net positive charge carried by the peptides. The presence of cholesterol in DMPG bilayers had no effect upon spectra of MGN-2a, MGN-2, or XFPa, which were identical to those seen in the presence of pure DMPG bilayers. Spectra of PGLa and PGL in DMPG/cholesterol were markedly different from those obtained in pure DMPG. For PGLa at low cholesterol concentrations (lipid:cholesterol ratio of 10:1), the major absorption was at 1648 cm^{-1} with a second band at 1637 cm^{-1} (Figure 2A) indicating adoption of a mostly helical secondary structure with some β elements, similar to spectra in pure DMPG. However, a significant absorption was also apparent at 1614 cm^{-1}. Absorptions in the range 1610–1629 cm^{-1} are highly characteristic of proteins and peptides that have aggregated and formed intermolecular hydrogen bonds (sometimes called an intermolecular β-sheet). Increasing the cholesterol content increased the intensity of this band. It therefore appears that the presence of cholesterol promotes aggregation of PGLa. Incorporation of cholesterol will have two significant effects upon the bilayer. First, the well-known fluidizing effect of cholesterol will disorder the bilayer. This disruption of the packing of the bilayer is not in itself sufficient to promote aggregation; otherwise aggregation would be apparent above the T_m in pure DMPG. Rather, the aggregation is likely the result of a second effect of cholesterol incorporation, that is, a change in the charge density at the liposome surface. The reduced surface charge density may be insufficient to allow full neutralization of the positively charged residues of the peptide and prevents adoption of an α-helical structure. Instead, the peptide is held at the surface by electrostatic interactions in an extended conformation. The hydrogen bond requirements of the peptide are then satisfied by the formation of intermolecular hydrogen bonds between neighboring peptide chains. Increasing the cholesterol content of the bilayer further decreases the charge density, more peptide molecules are held at the bilayer surface, and the band at 1614 cm^{-1} becomes stronger. The feature at 1628 cm^{-1} may have two possible origins. It may arise from intramolecular β-sheet structures, similar to those seen in the absence of cholesterol but with stronger hydrogen bonds, which reduce the frequency. However, it has been our experience that features below 1630 cm^{-1} generally arise from aggregated peptide chains. Thus, we suggest that this feature may reflect aggregation accompanied by formation of weak intermolecular hydrogen bonds. Such a situation would be expected to occur for polypeptide chains which retain some secondary structure, preventing close alignment of chains. It is therefore possible that two types of aggregate exist at the bilayer surface, one with very closely

aligned chains and a second with less well-aligned chains due to the presence of residual secondary structure.

Interestingly, while XPFa and PGLa share considerable sequence homology and a similar charge, only PGLa shows this unusual behavior with cholesterol-containing membranes. This implies not only that the amino acid sequence and net charge are important in governing peptide interactions but also that the distribution of the charge is important.

Removal of the terminal amide group significantly altered the interaction of PGL with DMPG/cholesterol bilayers (Figure 4). In pure DMPG bilayers, the peptide adopted a predominantly helical conformation with some β-sheet. In the presence of cholesterol, a marked increase in the β-sheet content was apparent as indicated by an increase in the intensity of the band at 1637 cm^{-1}. A band at 1665 cm^{-1} probably reflects contributions from turns. A small degree of aggregation is suggested by the presence of a weak feature at 1625 cm^{-1}. Thus, while cholesterol induces formation of intermolecular β-sheet in PGLa (as deduced from the highly characteristic absorption at 1614 cm^{-1}), the absorption at 1637 cm^{-1} in PGL suggests the effect is to induce intramolecular β-sheet.

Interaction of each peptide with SDS micelles was also demonstrated. Spectra of MGN-2a, XPFa, and MGN-2 were similar to those seen in DMPG bilayers. For PGLa and PGL this interaction resulted in the formation of helices and β-sheet as in DMPG, but with a drastic reduction in the intensity of the amide I band (Figure 2B). The reason for this reduction in intensity is unclear at this time. Addition of 100 mM cholesterol restored the intensity of the amide I band with the retention of the helical and β-sheet secondary structures. Similar results were obtained with DMPA and DMPA/cholesterol liposomes.

In the above discussion, we have addressed the question of the structure of the magainin family of peptides in a range of environments. It now remains for the structure of the peptides to be related to function. A negatively charged membrane-induced conformational change has been demonstrated in each peptide. However, the magainin peptides are relatively short, and may not be able to completely span a bilayer. Magainins have been shown to polymerize into long filaments upon lowering the pH and increasing the salt concentration of solutions (Urrutia et al., 1989). Thus, there is evidence that the peptides can form structures of sufficient length to span the bacterial cell wall of both Gram-positive and Gram-negative organisms. We therefore propose the following mechanism for the antimicrobial activity of magainins. As a response to noxious stimuli, the granular glands in the frog skin secrete the peptides in a disordered conformation. Upon contact with bacteria, the peptides interact with the negatively charged lipids of the bacterial outer membrane (Rana et al., 1990, 1991). The resulting charge neutralization allows a conformational rearrangement such that the peptides now adopt a predominantly helical secondary structure. The helix, or possibly a filament formed by the polymerization of the peptide, then penetrates the bacterial membrane. The amphipathic peptide then aggregates in the membrane to form ion channels, which disrupt the electrochemical gradient across the membranes of the cell and cause cell death (Westerhoff et al., 1990). Polymerization of the peptides to form long filaments may allow these relatively-short peptides to completely span the cell wall membranes of bacteria.

ACKNOWLEDGMENT

We thank Dr. Zhuying Dai for assistance with the antibacterial assays.

REFERENCES

Andreu, D., Aschauer, H., Kreil, G., & Merrifield, R. B. (1985) *Eur. J. Biochem. 149*, 531.
Bevins, C. L., & Zasloff, M. (1990) *Annu. Rev. Biochem. 59*, 395.
Byler, D. M., & Susi, H. (1988) *Biopolymers 25*, 469.
Chen, H.-C., Brown, J. H., Morell, J. L., & Huang, C. M. (1988) *FEBS Lett. 236*, 462.
Chen, H.-C., Brown, J. H., Morell, J. L., & Huang, C. M. (1990) in *Peptides: Chemistry, Structure and Biology* (Rivier, J. E., & Marshall, G. R., Eds.) p 122, Escom, Leiden, The Netherlands.
Cuervo, J. H., Rodriguez, B., & Houghton, R. A. (1990) in *Peptides: Chemistry, Structure and Biology* (Rivier, J. E., & Marshall, G. R., Eds.) p 124, Escom, Leiden, The Netherlands.
Duclohier, H., Molle, G., & Spach, G. (1989) *Biophys. J. 56*, 1017.
Gibson, B. W., Poulter, L., Williams, D. H., & Maggio, J. E. (1986) *J. Biol. Chem. 261*, 5341.
Giovannini, M. G., Poulter, L., Gibson, B. W., & Williams, D. H. (1987) *Biochem. J. 243*, 113.
Jackson, M., Haris, P. I., & Chapman, D. (1989) *J. Mol. Struct. 214*, 329.
Juretic, D., Chen, H.-C., Brown, J. H., Morell, J. L., Hendler, R. W., & Westerhoff, H. V. (1989) *FEBS Lett. 249*, 219.
Kennedy, D. F., Crisma, M., Toniolo, C., & Chapman, D. (1991) *Biochemistry 30*, 6541.
King, D. S., Fields, C. G., & Fields, G. B. (1990) *Int. J. Pept. Protein Res. 36*, 255.
Mantsch, H. H., Moffatt, D. J., & Casal, H. L. (1988) *J. Mol. Struct. 173*, 285.
Marion, D., Zasloff, M., & Bax, A. (1988) *FEBS Lett. 227*, 21.
Matsuzaki, K., Harada, M., Handa, T., Funakoshi, S., Fujii, N., Yajima, H., & Miyajima, K. (1989) *Biochim. Biophys. Acta 981*, 130.
Prestrelski, S. J., Byler, D. M., & Thompson, M. P. (1991) *Int. J. Pept. Protein Res. 37*, 508.
Rana, F. R., Sultany, C. M., & Blazyk, J. (1990) *FEBS Lett. 261*, 464.
Rana, F. R., Macais, E. A., Sultany, C. M., Modzrakowski, M. C., & Blazyk, J. (1991) *Biochemistry 30*, 5858.
Soravia, E., Martini, E., & Zasloff, M. (1988) *FEBS Lett. 228*, 337.
Surewicz, W. K., & Mantsch, H. H. (1988) *Biochim. Biophys. Acta 952*, 115.
Surewicz, W. K., & Mantsch, H. H. (1989) *J. Mol. Struct. 241*, 143.
Urrutia, R., Cruciani, R. A., Barker, J. L., & Kachar, B. (1989) *FEBS Lett. 247*, 17.
Westerhoff, H. V., Juretic, D., Hendler, R. W., & Zasloff, M. (1989) *Proc. Natl. Acad. Sci. U.S.A. 86*, 6597.
Williams, R. W., Covel, D., & Chen, H.-C. (1989) *J. Cell. Biochem., Suppl. 13A*, 96.
Williams, R. W., Starman, R., Taylor, K. M. P., Gable K., Beeler, T., Zasloff, M., & Covel, D. (1990) *Biochemistry 29*, 4490.
Zasloff, M. (1987) *Proc. Natl. Acad. Sci. U.S.A. 84*, 5449.
Zasloff, M., Martin, B., & Chen, H.-C. (1988) *Proc. Natl. Acad. Sci. U.S.A. 85*, 910.